

Non-classical correlations in a two-mode optomechanical system

J. El Qars^{a1}, M. Daoud^{b,c,d2} and R. Ahl Laamara^{a,e 3}

^a*LPHE-MS, Faculty of Sciences, University Mohammed V, Rabat, Morocco*

^b*Max Planck Institute for the Physics of Complex Systems, Dresden, Germany*

^c*Abdus Salam International Centre for Theoretical Physics, Miramare, Trieste, Italy*

^d*Department of Physics, Faculty of Sciences, University Ibnou Zohr, Agadir, Morocco*

^e*Centre of Physics and Mathematics (CPM), University Mohammed V, Rabat, Morocco*

Abstract

The pairwise quantum correlations in a tripartite optomechanical system comprising a mechanical mode and two optical modes are analyzed. The Simon criterion is used as a witness of the separability. Whereas, the Gaussian discord is employed to capture the quantumness of correlations. Both entanglement and Gaussian discord are evaluated as functions of the parameters characterizing the environment and the system (temperature, squeezing and optomechanical coupling). We work in the resolved-sideband regime. We show that it is possible to reach simultaneous three bipartite entanglements via the quantum correlations transfer from the squeezed light to the system. While, even without squeezed light, the quantumness of correlations can be captured simultaneously between the three modes for a very wide range of parameters. Specifically, we find that the two optical modes exhibit more quantum correlations in comparison with the entangled mechanical-optical modes. Finally, unlike the two hybrid subsystems, the purely optical one seems more resilient against the environmental destructive effects.

¹email: j.elqars@gmail.com

²email: m_daoud@hotmail.com

³email: ahllaamara@gmail.com

1 Introduction

In quantum information science, the study of quantum correlations is a key issue. In fact, the entanglement property in multipartite quantum systems is a fundamental resource for various quantum tasks [1]. In this context, quantifying quantum correlations has been the subject of extensive investigation during the last two decades. A particular attention was dedicated to entangled states of continuous variables systems, especially Gaussian states. Indeed, motivated by the experimental implementation and control of this kind of quantum states, a complete qualitative and quantitative characterization of the non-classical properties was obtained in the literature [2, 3, 4, 5, 6, 7, 8]. Moreover, the separability of two modes continuous variables (CVs) can be completely characterized using the Simon criterion [2]. We note that now it is clearly understood that separable states, especially mixed ones, might also contain quantum correlations and the separability is not an indicator of classicality. Thus, quantum discord has drawn much attention in recent years as the most used quantifier to capture the *quantumness* of correlations in discrete variables systems [9] as well as continuous variables (CVs) [10, 11]. In either Markovian or non-Markovian regimes, a considerable efforts have been devoted to investigate both entanglement and the Gaussian quantum discord in many different models [12, 13, 14, 15]. Essentially, it has been shown that unlike entanglement, quantum discord is more robust against the effects of the environment and interestingly, it is immune to sudden death [13, 14, 16, 17].

Encoding quantum information in quantum states of any realistic system encounters both the quantum decoherence and dissipation induced by the unavoidable coupling with its environment. In addition, a fairly good understanding of how to control the coupling between the quantum systems and their own environment, will make the exploitation of quantum properties for quantum information processing more effective. In this sense, there has been considerable interest in studying both decoherence and dissipation process, which are fundamental issues in quantum physics to understand the transition between classical and quantum worlds [18, 19].

Recently, significant efforts has been deployed towards the macroscopic quantum state by developing various schemes for their experimental production. In this context, quantum optomechanical systems constitute a promising candidate to investigate quantum mechanical effects [20]. Proposals include the ground state optical cooling of the fundamental mechanical mode [21, 22, 23], the creation of macroscopic quantum superpositions or so-called Schrödinger's cat states [24], quantum state transfer [25], the detection of the gravitational waves [26], entangling states of mechanical modes to each other [13, 27, 28, 29] or optical modes [30, 31], the entanglement generation between two optical modes [32, 33]. Now, it is more or less accepted that the encoding information in optomechanical systems can constitute a promising candidate in the field of quantum information science.

We consider an optomechanical setup where a movable mirror is placed inside a Fabry-Perot cavity. The analysis of the entanglement in such tripartite optomechanical system, where a single mechanical mode is coupled to two optical cavities modes via radiation pressure, was studied in Ref [34], knowing that no further approximation has been done apart from the linearization around the classical steady

state. The aim of the present work is to go one step further. Indeed, feeding the same optomechanical system by two-mode squeezed light and using the rotating wave approximation (RWA), we shall study the quantum correlations behavior between the different modes of the system. We use the Simon criterion as a witness of the separability [2] and we will extend our analyses far beyond entanglement trying to detect *the quantumness* of pairwise correlations in three different subsystems using the Gaussian quantum discord [10, 11].

The organization of this paper is as follows. In section 2, we introduce the basic model, give the quantum Langevin equations describing the dynamics of the single mechanical mode and the two optical modes. The needed approximations to get the explicit form of the covariance matrix are also discussed. In section 3, using the Simon criterion, the bi-separability between any pair of modes is studied in terms of the temperature to understand the thermal effects on the entanglement properties of the system. We also investigate the behavior of the entanglements under both the squeezing and the optomechanical coupling effects. In section 4, we investigate the quantum correlations in the system far beyond entanglement. For this, the pairwise Gaussian quantum discord among the three bipartite subsystems are computed and analyzed. Concluding remarks close this paper.

2 Formulation and theoretical description of the system

2.1 Model

The system under study, illustrated in Fig. 1, is a Fabry-Perot double-cavity system comprising one movable perfectly reflecting mirror, which is inserted between two fixed partially transmitting mirrors. The movable mirror is coupled simultaneously by means of radiation pressure to the right (respectively. left) optical cavity mode of frequency ω_{c_1} (respectively. ω_{c_2}). Each optical cavity mode (labeled as o_j for $j = 1, 2$) is driven by an external coherent laser source with the input power P_j , phase φ_j and frequency ω_{L_j} . In addition, we assume that the system is pumped by two-mode squeezed light produced for example by spontaneous parametric down-conversion source (SPDC) [35]. The first (respectively, second) squeezed mode is sent towards the right (respectively. left) side cavity. Finally, the movable mirror will be modeled as a quantum mechanical harmonic oscillator having an effective mass m_μ , a mechanical frequency denoted by ω_μ and a mechanical damping rate γ_μ .

In a frame rotating at the frequency ω_{L_j} ($j = 1, 2$) of the lasers, the Hamiltonian describing the optomechanical system under consideration can be written as [36]

$$H = \omega_\mu b^\dagger b + \sum_{j=1}^2 \left((\omega_{c_j} - \omega_{L_j}) a_j^\dagger a_j + (-1)^j g_j a_j^\dagger a_j (b^\dagger + b) + \varepsilon_j (a_j^\dagger e^{i\varphi_j} + a_j e^{-i\varphi_j}) \right). \quad (1)$$

As mentioned above, the movable mirror will be treated as a single mechanical mode (labeled as m) defined by the annihilation and creation operators b, b^\dagger with $[b, b^\dagger] = 1$. We denote by a_j and a_j^\dagger the annihilation and creation operators of the j^{th} optical cavity mode with $[a_j, a_k^\dagger] = \delta_{jk}$ (for $j, k = 1, 2$). The optomechanical single-photon coupling rate g_j between the mechanical mode and the j^{th} optical

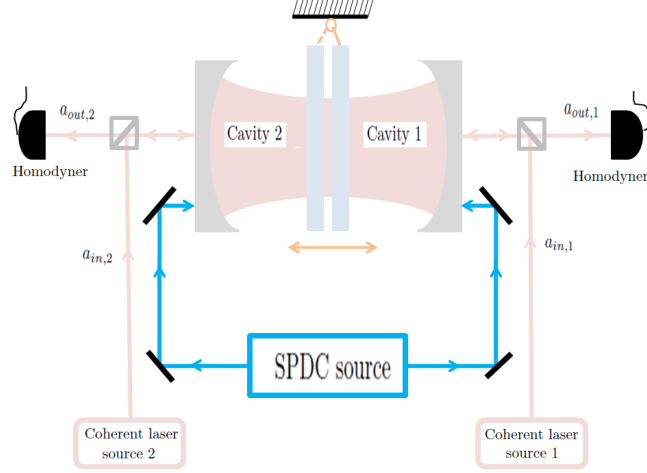


Figure 1: Schematic description of a double-cavity optomechanical system. The movable mirror which is represented as a mass on a pendulum with the mechanical frequency ω_μ , the damping rate γ_μ and an effective mass m_μ is modeled as a quantum mechanical harmonic oscillator. The system is injected simultaneously by two-mode squeezed light and coherent laser fields through the two partially transmitting mirrors. In addition, $a_{in,j}$ (respectively, $a_{out,j}$) represents the j^{th} input (respectively, the j^{th} output) laser field with $j = 1, 2$. By means of the homodyner systems, it is possible to evaluate numerically $a_{out,1}$ and $a_{out,2}$ which allows us to obtain the correlation matrix of the global system. Subsequently, one can compute both the entanglement and the Gaussian quantum discord in different bipartite subsystems.

cavity mode is given by $g_j = (\omega_{c_j}/l_j) (\hbar/m_\mu\omega_\mu)^{1/2}$. The quantities l_j stands for the j^{th} cavity length (with $j = 1, 2$). While, the coupling strength between the j^{th} external laser and its corresponding cavity field is defined by $\varepsilon_j = (2\kappa_j P_j/\hbar\omega_{L_j})^{1/2}$ (for $j = 1, 2$), where κ_j referring to the energy decay rate of the j^{th} cavity.

2.2 Quantum Langevin equations

In the Heisenberg picture, the dynamics of the mechanical mode and the j^{th} optical cavity mode is completely described by the following set of nonlinear quantum Langevin equations

$$\partial_t b = -\left(\frac{\gamma_\mu}{2} + i\omega_\mu\right)b + \sum_{j=1}^2 (-1)^{j+1} i g_j a_j^\dagger a_j + \sqrt{\gamma_\mu} b^{in}, \quad (2)$$

$$\partial_t a_j = -\left(\frac{\kappa_j}{2} - i\Delta_j\right)a_j + (-1)^{j+1} i g_j a_j (b^\dagger + b) - i\varepsilon_j e^{i\varphi_j} + \sqrt{\kappa_j} a_j^{in} \quad \text{for } j = 1, 2 \quad (3)$$

where $\Delta_j = \omega_{L_j} - \omega_{c_j}$ (for $j = 1, 2$) is the j^{th} laser detuning [20]. Moreover, b^{in} is the random Brownian operator with zero-mean value ($\langle b^{in} \rangle = 0$) describing the coupling of the movable mirror with its own environment. In general, b^{in} is not δ -correlated [37]. However, quantum effects are reached only using oscillators with a large mechanical quality factor $\mathcal{Q} = \omega_\mu/\gamma_\mu \gg 1$, which allowing us to recover the

Markovian process. In this limit, we have the following nonzero time-domain correlation functions [38]

$$\langle b^{in}(t)b^{in\dagger}(t') \rangle = (n_{\text{th}} + 1)\delta(t - t'), \quad (4)$$

$$\langle b^{in\dagger}(t)b^{in}(t') \rangle = n_{\text{th}}\delta(t - t'), \quad (5)$$

where $n_{\text{th}} = \left(\exp(\hbar\omega_\mu/k_B T) - 1 \right)^{-1}$ is the mean thermal photons number, T is the temperature of the mirror environment and k_B is the Boltzmann constant. Another kind of noise affecting the system is the j^{th} input squeezed vacuum noise operator a_j^{in} ($j = 1, 2$) with zero mean value. They satisfy the following non zero time-domain correlation properties given by [13, 29, 39]

$$\langle a_j^{in}(t)a_j^{in\dagger}(t') \rangle = (N + 1)\delta(t - t') \quad j = 1, 2, \quad (6)$$

$$\langle a_j^{in\dagger}(t)a_j^{in}(t') \rangle = N\delta(t - t') \quad j = 1, 2, \quad (7)$$

$$\langle a_j^{in\dagger}(t)a_k^{in\dagger}(t') \rangle = M e^{i\omega_\mu(t+t')} \delta(t - t') \quad k \neq j = 1, 2, \quad (8)$$

$$\langle a_j^{in}(t)a_k^{in}(t') \rangle = M e^{-i\omega_\mu(t+t')} \delta(t - t') \quad k \neq j = 1, 2, \quad (9)$$

with $N = \sinh^2 r$, $M = \sinh r \cosh r$ where r being the squeezing parameter.

2.3 Linearization of quantum Langevin equations

Due to the nonlinear nature of the radiation pressure, the investigation of the exact quantum dynamics of the whole system is non trivial, which subsequently makes impossible to get a rigorous analytical solutions of Eqs. (2) and (3). To overcome this difficulty, we adopt the linearization approach discussed in [40]. Indeed, in order to attain satisfactory levels of optomechanical interaction which leads to a stationary and robust entanglement, the two cavities should be intensely driven by strong power lasers so that the intra-cavities fields are strong. Assuming this, the steady-state mean value of each bosonic operator is larger in comparison with the corresponding fluctuation, i.e., $|\langle a_j \rangle| = |a_{js}| \gg |\delta a_j|$ for $j = 1, 2$ and $|\langle b \rangle| = |b_s| \gg |\delta b|$. In this sense, we consider the dynamics of small fluctuations around the steady state of the system by decomposing each operator (b , a_1 and a_2) into two parts, i.e., sum of its mean value and a small fluctuation with zero mean value ($\langle \delta a_j \rangle = 0$ for $j = 1, 2$ and $\langle \delta b \rangle = 0$), so

$$b = b_s + \delta b, \quad a_j = a_{js} + \delta a_j \quad \text{for } j = 1, 2, \quad (10)$$

where the mean values b_s and a_{js} (for $j = 1, 2$) are complex-numbers and can be evaluated by setting the time derivatives to zero and factorizing the averages in Eqs. (2) and (3). Thus, the steady-state values b_s and a_{js} write as

$$b_s = \frac{2i}{\gamma_\mu + 2i\omega_\mu} \sum_{j=1}^2 (-1)^{j+1} g_j |a_{js}|^2, \quad (11)$$

$$a_{js} = -2ie^{i\varphi_j} \frac{\varepsilon_j}{\kappa_j - 2i\Delta'_j} \quad \text{for } j = 1, 2, \quad (12)$$

where $\Delta'_j = \Delta_j + (-1)^{j+1} g_j (b_s^* + b_s)$ is the j^{th} effective cavity detuning including the radiation pressure effects [20, 41]. When the two cavities are intensely driven so that the intracavities fields are strong,

i.e., $|a_{js}| \gg 1$ for $j = 1, 2$, the nonlinear terms $\delta a_j^\dagger \delta a_j$, $\delta a_j \delta b$ and $\delta a_j \delta b^\dagger$ (for $j = 1, 2$), can be safely neglected. Hence, one gets the following linearized Langevin equations

$$\partial_t \delta b = -\left(i\omega_\mu + \frac{\gamma_\mu}{2}\right) \delta b + \sum_{j=1}^2 (-1)^j \mathcal{G}_j \left(\delta a_j - \delta a_j^\dagger\right) + \sqrt{\gamma_\mu} b^{in}, \quad (13)$$

$$\partial_t \delta a_j = -\left(\frac{\kappa_j}{2} - i\Delta'_j\right) \delta a_j + (-1)^{j+1} \mathcal{G}_j \left(\delta b^\dagger + \delta b\right) + \sqrt{\kappa_j} a_j^{in} \quad \text{for } j = 1, 2. \quad (14)$$

In the two last equations, the parameter \mathcal{G}_j (for $j = 1, 2$) defined by $\mathcal{G}_j = g_j |a_{js}| = g_j \sqrt{\bar{n}_{\text{cav}}^j}$ is the j^{th} light-enhanced optomechanical coupling for the linearized regime [20]. While, the quantity \bar{n}_{cav}^j represents the number of photons circulating inside the j^{th} cavity [20]. Using the bosonic linearization (10), the Hamiltonian (1) can be rewritten as

$$H_{eff} = \omega_\mu \delta b^\dagger \delta b + \sum_{j=1}^2 \left[(-1)^{j+1} \Delta'_j \delta a_j^\dagger \delta a_j + i(-1)^j \mathcal{G}_j (\delta a_j - \delta a_j^\dagger) (\delta b + \delta b^\dagger) \right], \quad (15)$$

where \mathcal{G}_j can be interpreted as a new j^{th} effective optomechanical coupling. In fact, it is simple to see that the linearized quantum Langevin equations (13) and (14) can be directly obtained from the effective Hamiltonian (15). One can verify that the operators δa_j and δb satisfy the usual bosonic commutations rules (i.e. $[\delta a_j, \delta a_j^\dagger] = [\delta b, \delta b^\dagger] = 1$, $[\delta a_j, H_{eff}] \sim \delta a_j$ and $[\delta b, H_{eff}] \sim \delta b$). We highlight that the Eqs. (13), (14) and (15) have been obtained by setting $a_{js} = -i|a_{js}|$ or equivalently by taking the phase φ_j of the j^{th} input laser field equal to $\varphi_j = -\arctan(2\Delta'_j/\kappa_j)$ [42]. Now, we introduce the operators $\tilde{\delta b}$ and $\tilde{\delta a}_j$ defined by $\delta b = \tilde{\delta b} e^{-i\omega_\mu t}$ and $\delta a_j = \tilde{\delta a}_j e^{i\Delta'_j t}$ (for $j = 1, 2$) and using the Eqs. (13) and (14), one has

$$\partial_t \tilde{\delta b} = -\frac{\gamma_\mu}{2} \tilde{\delta b} + \sum_{j=1}^2 (-1)^j \mathcal{G}_j \left(\tilde{\delta a}_j e^{i(\omega_\mu + \Delta'_j)t} - \tilde{\delta a}_j^\dagger e^{i(\omega_\mu - \Delta'_j)t} \right) + \sqrt{\gamma_\mu} \tilde{b}^{in}, \quad (16)$$

$$\partial_t \tilde{\delta a}_j = -\frac{\kappa_j}{2} \tilde{\delta a}_j + (-1)^{j+1} \mathcal{G}_j \left(\tilde{\delta b} e^{-i(\omega_\mu + \Delta'_j)t} + \tilde{\delta b}^\dagger e^{i(\omega_\mu - \Delta'_j)t} \right) + \sqrt{\kappa_j} \tilde{a}_j^{in} \quad \text{for } j = 1, 2. \quad (17)$$

Next, we assume that the two cavities are driven at *the red sideband* ($\Delta'_j = -\omega_\mu$ for $j = 1, 2$) which corresponds to the quantum states transfer [28, 43] (we recall that the j^{th} laser detuning Δ_j has been defined as $\Delta_j = \omega_{L_j} - \omega_{c_j}$). Further, in the resolved-sideband regime, where the mechanical frequency ω_μ of the movable mirror is much larger than the j^{th} cavity decay rate κ_j ($\omega_\mu \gg \kappa_1, \kappa_2$), one can use the rotating wave approximation (RWA) [20, 44]. Therefore, ignoring the fast oscillating terms which rotating at the frequencies $\pm 2\omega_\mu$ in Eqs. (16) and (17), one gets

$$\partial_t \tilde{\delta b} = -\frac{\gamma_\mu}{2} \tilde{\delta b} + \sum_{j=1}^2 (-1)^j \mathcal{G}_j \tilde{\delta a}_j + \sqrt{\gamma_\mu} \tilde{b}^{in}, \quad (18)$$

$$\partial_t \tilde{\delta a}_j = -\frac{\kappa_j}{2} \tilde{\delta a}_j + (-1)^{j+1} \mathcal{G}_j \tilde{\delta b} + \sqrt{\kappa_j} \tilde{a}_j^{in} \quad \text{for } j = 1, 2. \quad (19)$$

We note that under the rotating wave approximation (RWA) with $\Delta'_{1,2} = -\omega_\mu$, Eq. (15) reduces to the following simple expression

$$H_{eff}^{\text{RWA}} = i \sum_{j=1}^2 (-1)^j \mathcal{G}_j \left[\delta a_j \delta b^\dagger - \delta a_j^\dagger \delta b \right], \quad (20)$$

from which one can derive the equations (18) and (19).

2.4 Covariance matrix and Lyapunov equation

In order to investigate the bipartite quantum correlations between the different modes of the whole system, it is more convenient to transform Eqs. (18) and (19) in terms of the quadratures operators of the three Gaussian modes (two optical modes and a single mechanical mode) and their corresponding Hermitian input noise operators. Thus, for the two optical cavities modes, we introduce

$$\delta\tilde{X}_j = (\delta\tilde{a}_j^\dagger + \delta\tilde{a}_j)/\sqrt{2} \quad \text{and} \quad \delta\tilde{Y}_j = i(\delta\tilde{a}_j^\dagger - \delta\tilde{a}_j)/\sqrt{2} \quad \text{for } j = 1, 2, \quad (21)$$

$$\tilde{X}_j^{in} = (\tilde{a}_j^{in\dagger} + \tilde{a}_j^{in})/\sqrt{2} \quad \text{and} \quad \tilde{Y}_j^{in} = i(\tilde{a}_j^{in\dagger} - \tilde{a}_j^{in})/\sqrt{2} \quad \text{for } j = 1, 2. \quad (22)$$

In a similar way, we define for the single mechanical mode

$$\delta\tilde{q} = (\delta\tilde{b}^\dagger + \delta\tilde{b})/\sqrt{2} \quad \text{and} \quad \delta\tilde{p} = i(\delta\tilde{b}^\dagger - \delta\tilde{b})/\sqrt{2}, \quad (23)$$

$$\tilde{q}^{in} = (\tilde{b}^{in\dagger} + \tilde{b}^{in})/\sqrt{2} \quad \text{and} \quad \tilde{p}^{in} = i(\tilde{b}^{in\dagger} - \tilde{b}^{in})/\sqrt{2}. \quad (24)$$

It is simple to check that the fluctuations of the quadratures operators satisfy the following set of linear quantum Langevin equations

$$\partial_t \delta\tilde{X}_j = -\frac{\kappa_j}{2} \delta\tilde{X}_j + (-1)^{j+1} \mathcal{G}_j \delta\tilde{q} + \sqrt{\kappa_j} \tilde{X}_j^{in} \quad \text{for } j = 1, 2, \quad (25)$$

$$\partial_t \delta\tilde{Y}_j = -\frac{\kappa_j}{2} \delta\tilde{Y}_j + (-1)^{j+1} \mathcal{G}_j \delta\tilde{p} + \sqrt{\kappa_j} \tilde{Y}_j^{in} \quad \text{for } j = 1, 2, \quad (26)$$

$$\partial_t \delta\tilde{q} = \sum_{j=1}^2 (-1)^j \mathcal{G}_j \delta\tilde{X}_j - \frac{\gamma_\mu}{2} \delta\tilde{q} + \sqrt{\gamma_\mu} \tilde{q}^{in}, \quad (27)$$

$$\partial_t \delta\tilde{p} = \sum_{j=1}^2 (-1)^j \mathcal{G}_j \delta\tilde{Y}_j - \frac{\gamma_\mu}{2} \delta\tilde{p} + \sqrt{\gamma_\mu} \tilde{p}^{in}. \quad (28)$$

Using the observables δX_j , δY_j , δq and δp defined by (21) and (23), the Hamiltonian (20) becomes

$$\mathcal{H}_{eff} = \sum_{j=1}^2 (-1)^j \mathcal{G}_j [\delta X_j \delta p - \delta Y_j \delta q], \quad (29)$$

leading to linearized quantum Langevin equations (25)-(28). These equations can be written in the following compact matrix form

$$\partial_t u = Au + n, \quad (30)$$

with $u = (\delta\tilde{X}_1, \delta\tilde{Y}_1, \delta\tilde{X}_2, \delta\tilde{Y}_2, \delta\tilde{q}, \delta\tilde{p})^T$ and $n = (\sqrt{\kappa_1} \tilde{X}_1^{in}, \sqrt{\kappa_1} \tilde{Y}_1^{in}, \sqrt{\kappa_2} \tilde{X}_2^{in}, \sqrt{\kappa_2} \tilde{Y}_2^{in}, \sqrt{\gamma_\mu} \tilde{q}^{in}, \sqrt{\gamma_\mu} \tilde{p}^{in})^T$ are respectively the column vector of quadratures fluctuations and the column vector of the noise sources. Moreover, the 6×6 matrix A in Eq. (30) represents the drift matrix of the system under investigation [21]. Introducing the j^{th} multiphoton optomechanical cooperativity \mathcal{C}_j defined as [20, 45]

$$\mathcal{C}_j = \frac{4\mathcal{G}_j^2}{\kappa_j \gamma_\mu} = \frac{4g_j^2 \bar{n}_{cav}^j}{\kappa_j \gamma_\mu} = \frac{8\omega_{c_j}^2}{\gamma_\mu m_\mu \omega_\mu \omega_{L_j} l_j^2} \frac{P_j}{\left[\left(\frac{\kappa_j}{2}\right)^2 + \omega_\mu^2\right]} \quad \text{for } j = 1, 2, \quad (31)$$

the drift matrix A can be expressed as

$$A = \frac{1}{2} \begin{pmatrix} -\kappa_1 & 0 & 0 & 0 & \sqrt{\gamma_\mu \kappa_1 \mathcal{C}_1} & 0 \\ 0 & -\kappa_1 & 0 & 0 & 0 & \sqrt{\gamma_\mu \kappa_1 \mathcal{C}_1} \\ 0 & 0 & -\kappa_2 & 0 & -\sqrt{\gamma_\mu \kappa_2 \mathcal{C}_2} & 0 \\ 0 & 0 & 0 & -\kappa_2 & 0 & -\sqrt{\gamma_\mu \kappa_2 \mathcal{C}_2} \\ -\sqrt{\gamma_\mu \kappa_1 \mathcal{C}_1} & 0 & \sqrt{\gamma_\mu \kappa_2 \mathcal{C}_2} & 0 & -\gamma_\mu & 0 \\ 0 & -\sqrt{\gamma_\mu \kappa_1 \mathcal{C}_1} & 0 & \sqrt{\gamma_\mu \kappa_2 \mathcal{C}_2} & 0 & -\gamma_\mu \end{pmatrix}. \quad (32)$$

We note that a weaker condition to reach the regime of strong optomechanical coupling is given by $\mathcal{C}_j \gg 1$ (for $j = 1, 2$) [46]. The solution of Eq. (30) can be written as [29, 30]

$$u(t) = F(t)u(0) + \int_0^t ds F(s)n(t-s), \quad (33)$$

with $F(t) = \exp\{At\}$. The system is stable and reaches its steady state if and only when the real parts of all the eigenvalues of the drift-matrix A are negative, thus $F(\infty) = 0$. The stability conditions of the system can be obtained using the Routh–Hurwitz criterion [47]. Due to the 6×6 dimension of the drift matrix A (see Eq. (32)), the explicit expressions of the stability conditions are quite cumbersome and will not be reported here. We emphasize that all the parameters chosen in this paper have been verified to satisfy the stability conditions.

The quantum operators noises a_j^{in} and b^{in} are zero-mean quantum Gaussian noises and the dynamics has been linearized (see Eqs. [(25)-(28)]). So, the steady state of the system is a zero-mean tripartite Gaussian state with zero mean fluctuations [48]. The system is completely specified by its 6×6 covariance matrix (CM) V [49], with matrix elements

$$V_{ii'} = (\langle u_i(\infty)u_{i'}(\infty) + u_{i'}(\infty)u_i(\infty) \rangle)/2, \quad (34)$$

where $u = \left(\delta\tilde{X}_1(\infty), \delta\tilde{Y}_1(\infty), \delta\tilde{X}_2(\infty), \delta\tilde{Y}_2(\infty), \delta\tilde{q}(\infty), \delta\tilde{p}(\infty) \right)^T$ is the vector of continuous variable fluctuation operators in the steady state ($t \rightarrow \infty$). We note that V is a real, symmetric, positive definite matrix [50]. When the system is stable and using Eq. (33), the covariance matrix elements write

$$V_{ii'} = \sum_{k,k'} \int_0^\infty ds \int_0^\infty ds' F_{ik}(s)F_{i'k'}(s')\Phi_{kk'}(s-s'), \quad (35)$$

where $\Phi_{kk'}(s-s') = (\langle n_k(s)n_{k'}(s') + n_{k'}(s')n_k(s) \rangle)/2 = D_{kk'}\delta(s-s')$ are the components of the diffusion matrix D of the stationary noise correlation functions [21]. Using the correlation properties of the noise operators given by the Eqs. [(4)-(9)], we obtain

$$D = \begin{pmatrix} \kappa_1(N + \frac{1}{2}) & 0 & \sqrt{\kappa_1\kappa_2}M & 0 & 0 & 0 \\ 0 & \kappa_1(N + \frac{1}{2}) & 0 & -\sqrt{\kappa_1\kappa_2}M & 0 & 0 \\ \sqrt{\kappa_1\kappa_2}M & 0 & \kappa_2(N + \frac{1}{2}) & 0 & 0 & 0 \\ 0 & -\sqrt{\kappa_1\kappa_2}M & 0 & \kappa_2(N + \frac{1}{2}) & 0 & 0 \\ 0 & 0 & 0 & 0 & \gamma_\mu(n_{\text{th}} + \frac{1}{2}) & 0 \\ 0 & 0 & 0 & 0 & 0 & \gamma_\mu(n_{\text{th}} + \frac{1}{2}) \end{pmatrix}. \quad (36)$$

From Eq. (35), the covariance matrix V writes also as

$$V = \int_0^\infty ds F(s) D F(s)^T. \quad (37)$$

When the system is stable ($F(\infty) = 0$), Eq. (37) is equivalent to the Lyapunov equation for the steady-state (CM) [51]

$$AV + VA^T = -D. \quad (38)$$

It is clear that the Eq. (38) is linear for V , thus it can be straightforwardly solved, but the explicit expression of V is too cumbersome and can not be reported here.

3 Bipartite and tripartite optomechanical entanglement

3.1 The Simon criterion as witness of entanglement

In the systems of continuous-variables (CVs), the investigation of the entanglement properties has been the object of study in a number of recent publications in bipartite systems [13, 27, 28, 29, 30, 31, 32, 33]. The quantum correlations in a tripartite optical system were reported in [52] and more recently many other proposals focused particularly into the field of optomechanics [34, 53, 54, 55, 56]. We notice that an interesting review of the theory of (CVs) entanglement was concisely given in [57]. The covariance matrix V which is solution of the Lyapunov equation (Eq. (38)), can be written in the 3×3 block following form

$$V = [V_{ii'}]_{6 \times 6} = \begin{pmatrix} B_{o_1} & C_{o_1 o_2} & C_{o_1 m} \\ C_{o_1 o_2}^T & B_{o_2} & C_{o_2 m} \\ C_{o_1 m}^T & C_{o_2 m}^T & B_m \end{pmatrix}, \quad (39)$$

where $B_{j'}$ is a 2×2 matrix that describes the local properties of the j' -mode. Whereas, $C_{j'j''}$ ($j' \neq j'' = o_1, o_2, m$) describes the intermode correlations. Thus, the reduced covariance matrix describing the correlations between j' and j'' modes is given by

$$[V_{j'j''}]_{4 \times 4} = \begin{pmatrix} B_{j'} & C_{j'j''} \\ C_{j'j''}^T & B_{j''} \end{pmatrix}. \quad (40)$$

Due to the Gaussian nature of the system under investigation, the bipartite entanglement between the two modes j' and j'' ($j' \neq j'' = o_1, o_2, m$) can be quantified in terms of the Simon's necessary and sufficient entanglement nonpositive partial transpose criterion of the Gaussian states [2]. According to this end, the two modes j' and j'' ($j' \neq j'' = o_1, o_2, m$) are entangled if and only if $\eta_{j'j''}^- < 1/2$. The smallest symplectic eigenvalue $\eta_{j'j''}^-$, which obtained by the partial transpose of the 4×4 covariance matrix Eq. (40) is given by [4, 7, 58]

$$\eta_{j'j''}^- = \sqrt{\frac{\Delta_{j'j''} - \sqrt{\Delta_{j'j''}^2 - 4 \det V_{j'j''}}}{2}}, \quad (41)$$

with $\Delta_{j'j''} = \det B_{j'} + \det B_{j''} - 2 \det C_{j'j''}$, where the three 2×2 submatrices $B_{j'}$, $B_{j''}$ and $C_{j'j''}$ can be extracted from Eq. (40).

3.2 Stationary bipartite and tripartite entanglement analysis

3.2.1 Entanglement analysis versus the thermal effect

We now analyze the stationary entanglement distribution among the three possible bipartite subsystems using the smallest symplectic eigenvalues $\eta_{j'j''}^-$ ($j' \neq j'' = o_1, o_2, m$) given by (41). In what follows, $\eta_{mo_1}^-$, $\eta_{mo_2}^-$ and $\eta_{o_1o_2}^-$ denote respectively the smallest symplectic eigenvalue witnesses the entanglement $m - o_1$ between the mechanical mode m and the optical mode o_1 , the entanglement $m - o_2$ between the mechanical mode m and the optical mode o_2 and finally, the entanglement $o_1 - o_2$ between the two optical cavities modes o_1 and o_2 . The behavior of the three bipartite entanglements have been analyzed under influence of the temperature T of the thermal bath of the movable mirror, the squeezing parameter r and also the optomechanical cooperativity \mathcal{C}_1 of the right cavity. For simplicity, we take all the two cavities parameters to be identical, except the j^{th} input power laser P_j , where we have fixed $P_2 = 2P_1$ (without loss of generality) or equivalently $\mathcal{C}_2 = 2\mathcal{C}_1$ (see Eq. (31)). We start with the influence of the temperature on the three entanglements. In order to do realistic estimation, we used parameters from recent optomechanical experiment [46]: the wavelength of the

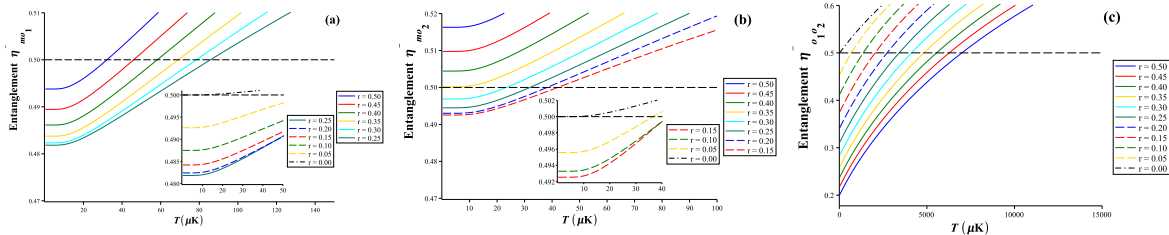


Figure 2: Mechanical bath temperature dependence of the smallest symplectic eigenvalue $\eta_{j'j''}^-$ used as a witness of the bipartite entanglement between, (a): the mechanical mode m and the optical mode o_1 , (b): the mechanical mode m and the optical mode o_2 , (c): the two optical modes o_1 and o_2 . All the two cavities parameters are identical, except the j^{th} input power laser P_j , where we have taken $P_2 = 2P_1$ or equivalently $\mathcal{C}_2 = 2\mathcal{C}_1$. In the panels (a), (b) and (c), each curve corresponds to a given value of the squeezing parameter r . The horizontal dashed line ($\eta_{j'j''}^- = 0.5$) represents the boundary between the entangled states $\eta_{j'j''}^- < 0.5$ and the others separable $\eta_{j'j''}^- > 0.5$. Unlike the two hybrid subsystems, significant entanglement is found over a wide range of temperatures in the purely optical subsystem (up to $T = 6.5$ mK for $r = 0.5$ in panel (c)). The two insets of panels (a) and (b) reveal the effect of low squeezing r on the $m - o_1$ and $m - o_2$ entanglements. We emphasize that, the energies decay rates $\kappa_{1,2}$, the mechanical damping rate γ_μ and the optomechanical cooperativity \mathcal{C}_1 are fixed respectively as $\kappa_{1,2} = 2\pi \times 215 \times 10^3$ Hz, $\gamma_\mu = 2\pi \cdot 1500$ Hz and $\mathcal{C}_1 = 35$.

lasers $\lambda_{1,2} = 1064$ nm so $\omega_{L_{1,2}} = 2\pi \times 2.82 \times 10^{14}$ Hz, $P_1 = 10$ mW ($P_2 = 2P_1 = 20$ mW), $l_{1,2} = 25$ mm, $\kappa_{1,2} = 2\pi \times 215 \times 10^3$ Hz, $\omega_\mu = 2\pi \times 947 \times 10^3$ Hz, $m_\mu = 145$ ng and $\omega_{c_{1,2}} \approx 3.5 \times 10^{15}$ Hz. For the mechanical damping rate γ_μ , we have used $\gamma_\mu \approx 2\pi \times 1.5 \times 10^3$ Hz, which is very comparable to the value that used in [59]. Next, using the explicit expression of the j^{th} optomechanical cooperativity \mathcal{C}_j given by Eq. (31), one has $\mathcal{C}_1 \approx 35$ so $\mathcal{C}_2 = 2\mathcal{C}_1 \approx 70$. The dependence of the three bipartite entanglements

$m - o_1$, $m - o_2$ and $o_1 - o_2$ on the mechanical bath temperature for various squeezing r is presented in Fig. 2. For a given squeeze r , as the environmental temperature increases, the amount of the $j' - j''$ entanglement monotonically decreases ($\eta_{j'j''}^-$ increases) due to the thermal fluctuations. Consequently, above a critical temperature T_c , the $j' - j''$ entanglement disappears completely as expected (T_c defined as: $T > T_c$, $\eta_{j'j''}^- > 1/2$ for a given squeeze r). Such a behavior is commonly known as *entanglement sudden death* (ESD) [60]. Comparing with the $m - o_1$ and $m - o_2$ entanglements, it can be clearly seen from Fig. 2 that the $o_1 - o_2$ entanglement is considerably large and more robust against the thermal noises enhanced by high temperatures and enough squeezing. Obviously, the panels (a), (b) and (c) in Fig. 2, show that for zero squeezing ($r = 0$), $\eta_{j'j''}^-$ is always upper than $1/2$ whatever T and regardless j' and j'' ($j' \neq j'' = o_1, o_2, m$), meaning that no entanglement occurs in any bipartite subsystem. Whereas, the two modes j' and j'' become entangled if we inject the squeezed light, indicating quantum fluctuations transfer from the two-mode squeezed light to the three subsystems. In addition, the two insets of panels (a) and (b) reveal that low values of the squeezing r enhance the entanglements $m - o_1$ and $m - o_2$. In contrast, high values of the squeezing r induce the entanglement degradation in the two hybrid subsystems. Finally, it is interesting to remark that for small values of T and r ($T < 20\mu\text{K}$, $0 < r < 0.3$), the three-bipartite entanglements $m - o_1$, $m - o_2$ and $o_1 - o_2$ can be observed simultaneously, which confirms the existence of strong correlations distribution between the three optomechanical modes.

3.2.2 Entanglement analysis versus the squeezing effect

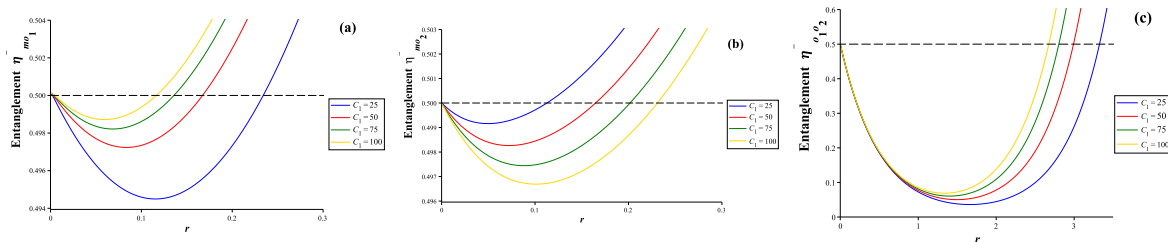


Figure 3: The three bipartite entanglements versus the squeezing parameter r for various values of the dimensionless optomechanical cooperativity \mathcal{C}_1 of the right cavity. As in Fig. 2, we have taken $\mathcal{C}_2 = 2\mathcal{C}_1$ and $\kappa_1 = \kappa_2 = 2\pi \times 215 \times 10^3$ Hz. The panels (a), (b) and (c) correspond respectively to the bipartite entanglement between : (a) the mechanical mode m and the optical mode o_1 ($\eta_{mo_1}^-$), (b) the mechanical mode m and the optical mode o_2 ($\eta_{mo_2}^-$) and finally, (c) the two optical modes o_1 and o_2 ($\eta_{o_1o_2}^-$). Here we used $\gamma_\mu = 2\pi \cdot 140$ Hz as a value of the mechanical damping rate [46]. For the mean thermal photons number n_{th} , we have used $n_{\text{th}} = 10^{-3}$ ($T \simeq 6.5 \mu\text{K}$). In the three panels (a), (b) and (c), the horizontal dashed line corresponds to $\eta_{j'j''}^- = 1/2$ below which the two modes ($j' - j''$) are entangled. This figure shows that the three entanglements $m - o_1$, $m - o_2$ and $o_1 - o_2$ have the resonance-like behavior with respect to the squeezing values r . Large entanglement has been detected up to $r \simeq 3.2$ in the purely optical subsystem for $\mathcal{C}_1 = 25$.

The squeezed light effect on the three bipartite entanglements $m - o_1$, $m - o_2$ and $o_1 - o_2$ quantified respectively by $\eta_{mo_1}^-$, $\eta_{mo_2}^-$ and $\eta_{o_1o_2}^-$ is presented in Fig. 3. For the mechanical damping rate γ_μ and the j^{th} energy decay rate κ_j , we have used respectively $\gamma_\mu = 2\pi \times 140$ Hz and $\kappa_1 = \kappa_2 = 2\pi \times 215 \times 10^3$ Hz [46]. For the mean thermal photons number n_{th} we used $n_{\text{th}} = 10^{-3}$ or equivalently $T \simeq 6.5$ μK . In the panels (a), (b) and (c), each curve corresponds to a given value of the optomechanical cooperativity \mathcal{C}_1 ($\mathcal{C}_2 = 2\mathcal{C}_1$). As depicted in the panels (a), (b) and (c), there would be no entanglement in any subsystem if $r = 0$. In addition, Fig. 3 reveals that the three bipartite entanglements $m - o_1$, $m - o_2$ and $o_1 - o_2$ have the resonance-like behavior with respect to the squeezing parameter r for a fixed value of \mathcal{C}_1 . Indeed, by increasing the squeezing parameter r , the three functions $\eta_{mo_1}^-$, $\eta_{mo_2}^-$ and $\eta_{o_1o_2}^-$ decrease gradually (the entanglements $m - o_1$, $m - o_2$ and $o_1 - o_2$ increase) reaching their minimum for a specific value of r denoted r_0 (r_0 depends both on the subsystem class and the fixed value of \mathcal{C}_1). Furthermore, for $r > r_0$ the functions $\eta_{mo_1}^-$, $\eta_{mo_2}^-$ and $\eta_{o_1o_2}^-$ increase with r (the entanglements $m - o_1$, $m - o_2$ and $o_1 - o_2$ decrease) and quickly become up to $1/2$, which corresponds to the entanglements degradation. The resonance-like behavior can be explicated as follows: for $0 < r < r_0$, the photons number in the two cavities increases, which enhances the optomechanical coupling by means of radiation pressure and consequently leads to robust entanglement [29]. In contrast, for $r > r_0$ the input thermal noise affecting each cavity becomes important and more aggressive causing the entanglement degradation [13]. More important, Fig. 3 shows that among the three bipartite entanglements $m - o_1$, $m - o_2$ and $o_1 - o_2$, the largest and robust one against the thermal noise enhanced by broadband squeezed light is also that between the two optical cavities modes, even though they are uncoupled.

3.2.3 Entanglement analysis versus the optomechanical coupling

We further illustrate in Fig. 4 the behavior of the three functions $\eta_{mo_1}^-$, $\eta_{mo_2}^-$ and $\eta_{o_1o_2}^-$ with respect to the dimensionless optomechanical cooperativity \mathcal{C}_1 ($\mathcal{C}_2 = 2\mathcal{C}_1$) and for various values of the squeezing parameter r . Here, we used $n_{\text{th}} = 10^{-2}$ (or equivalently $T \simeq 9.8$ μK) as value of the mean thermal photons number. The parameters γ_μ , κ_1 and κ_2 are the same as in Fig. 3. Focusing on the panels (a) and (b) in Fig. 4, it is clear that in the case of weak coupling $\mathcal{C}_1 \ll 1$ as well as in the strong coupling $\mathcal{C}_1 \gg 1$ (we note that, in the strong coupling limit, \mathcal{C}_1 can reach 10^6 [61]), the two optomechanical hybrid subsystems are separable ($\eta_{mo_1}^- > 1/2$ and $\eta_{mo_2}^- > 1/2$). In contrast, for the same values of the squeezing parameter r which have been used in panels (a), (b) of Fig. 4 (except $r = 0$), the two optical modes o_1 and o_2 remain always entangled regardless the coupling regime (see the inset (c'') of panel (c) in Fig. 4). Whereas, to observe the transition from the entangled states to the others separable in the purely optical subsystem, both broadband squeezed light and strong coupling regime are required. More interestingly, all the results obtained in Figs. 3, 4 and 5 show that, pumping the double-cavity system by the squeezed light is a necessary condition to attained bipartite and tripartite entanglement (for $r = 0$, the three functions $\eta_{mo_1}^-$, $\eta_{mo_2}^-$ and $\eta_{o_1o_2}^-$ are always upper or equal $1/2$ regardless the others circumstance). This can be interpreted as quantum correlations

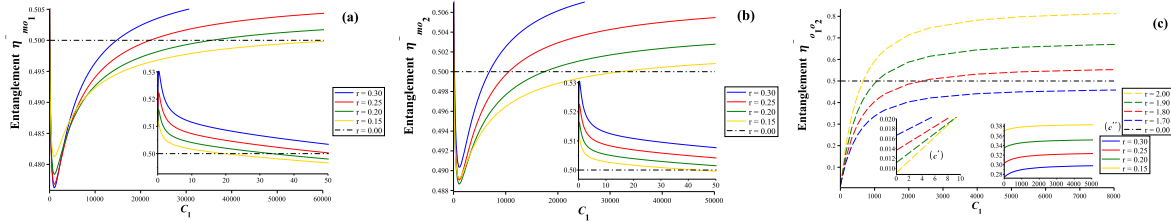


Figure 4: Plots of the three bipartite entanglements characterized by $\eta_{j'j''}^-$ ($j' \neq j'' = o_1, o_2, m$) as functions of the dimensionless optomechanical cooperativity \mathcal{C}_1 of the right cavity. \mathcal{C}_2 has been chosen to be $\mathcal{C}_2 = 2\mathcal{C}_1$ without loss of generality. Here we used $\kappa_1 = \kappa_2 = 2\pi \times 215 \times 10^3$ Hz, $\gamma_\mu = 2\pi \cdot 140$ Hz and $n_{\text{th}} = 10^{-2}$ ($T \simeq 9.8$ μK). Different graphs correspond to different values of the squeezing r . The panels (a), (b) and (c) represent successively the entanglement between: the mechanical mode m and the cavity mode o_1 ($\eta_{m o_1}^-$), the mechanical mode m and the cavity mode o_2 ($\eta_{m o_2}^-$) and finally, the two optical cavities modes o_1 and o_2 ($\eta_{o_1 o_2}^-$). In the two insets, we are zooming into the region where $\mathcal{C}_1 < 50$. As seen in the inset (c'') of panel (c), the purely optical subsystem remains always entangled for the same squeezing values which have been used in the panels (a) and (b) regardless the coupling regime. To switch from the entangled states to the others separable in the purely optical subsystem, both broadband squeezed light and strong coupling are required. For $r = 0$ which corresponds to the horizontal dotted-dashed line, the three subsystems are always separable whatever the value of \mathcal{C}_1 .

transfer from the two-mode squeezed light to the three bipartite subsystems. According also to the results obtained in Figs. 3, 4 and 5, we have shown that, in an experimentally accessible parameter regime, optomechanical entanglement can be reached *simultaneously* in the three bipartite subsystems, confirming the existence of strong quantum correlations distribution among the three modes. Finally, to close this section, we emphasize that in various circumstances governed either by T , r or \mathcal{C}_1 , the largest and robust stationary bipartite entanglement has been observed is the one between the two optical modes o_1 and o_2 which are indirectly coupled.

4 Quantum correlations beyond entanglement

4.1 Gaussian quantum discord

In this section, using the Gaussian quantum discord, we shall investigate the non-classical correlations behavior in the three bipartite subsystems $m - o_1$, $m - o_2$ and $o_1 - o_2$ far beyond entanglement. Recently, the Gaussian quantum discord has been introduced to be more general than entanglement as an indicator of non-classicality in (CV) systems. Indeed, for some systems which exhibit non zero degree of mixture, the Gaussian quantum discord can be non zero even at the separable state which is a marker of the quantumness of correlations. Unlike entanglement, it has been shown recently in a various publications that the Gaussian quantum discord is more robust against dissipation and noise [17, 62] and essentially, it does not undergo sudden death [13, 14, 17, 32].

For a given bipartite Gaussian state, the analytical expression of the Gaussian quantum discord is

given by [10, 11]

$$D^{j'j''} = f\left(\sqrt{\det B_{j''}}\right) - f\left(\nu_+^{j'j''}\right) - f\left(\nu_-^{j'j''}\right) + f\left(\sqrt{\epsilon^{j'j''}}\right), \text{ for } j' \neq j'' = o_1, o_2, m, \quad (42)$$

with $f(x) = (x + 1/2) \ln(x + 1/2) - (x - 1/2) \ln(x - 1/2)$. Using the covariance matrix given by Eq. (40), we define the following five symplectic invariants [7] $\alpha_{j'} = \det B_{j'}$, $\beta_{j''} = \det B_{j''}$, $\theta_{j'j''} = \det C_{j'j''}$, $\lambda_{j'j''} = \det V_{j'j''}$ and $\tilde{\Delta}_{j'j''} = \alpha_{j'} + \beta_{j''} + 2\theta_{j'j''}$. The nonpartially transposed symplectic eigenvalues $\nu_+^{j'j''}$ and $\nu_-^{j'j''}$ which are invariant under symplectic transformations are given by [4, 63]

$$\nu_{\pm}^{j'j''} = \sqrt{\frac{\tilde{\Delta}_{j'j''} \pm \sqrt{\tilde{\Delta}_{j'j''}^2 - 4 \det V_{j'j''}}}{2}}. \quad (43)$$

The explicit expression of the quantity $\epsilon^{j'j''}$ which has been appeared in Eq. (42) is defined by [10, 49].

$$\epsilon^{j'j''} = \begin{cases} \frac{2(\theta_{j'j''})^2 + (1/4 - \beta_{j''})(\alpha_{j'} - 4\lambda_{j'j''}) + 2|\theta_{j'j''}| \sqrt{(\theta_{j'j''})^2 + (1/4 - \beta_{j''})(\alpha_{j'} - 4\lambda_{j'j''})}}{4(1/4 - \beta_{j''})^2} & \text{if } d^{j'j''} \leq 0 \\ \frac{\alpha_{j'}\beta_{j''} - (\theta_{j'j''})^2 + \lambda_{j'j''} - \sqrt{(\theta_{j'j''})^4 + (\lambda_{j'j''} - \alpha_{j'}\beta_{j''})^2 - 2(\theta_{j'j''})^2(\alpha_{j'}\beta_{j''} + \lambda_{j'j''})}}{2\beta_{j''}} & \text{if } d^{j'j''} > 0 \end{cases}, \quad (44)$$

where the discriminant $d^{j'j''}$ is given by

$$d^{j'j''} = \left(\lambda_{j'j''} - \alpha_{j'}\beta_{j''}\right)^2 - \left(1/4 + \beta_{j''}\right)\left(\theta_{j'j''}\right)^2\left(\alpha_{j'} + 4\lambda_{j'j''}\right). \quad (45)$$

In Eq. (42), the term $f\left(\sqrt{\det B_{j''}}\right)$ is the Von-Neumann entropy of the reduced state of the j'' -mode. Whereas, the quantity $f\left(\nu_+^{j'j''}\right) + f\left(\nu_-^{j'j''}\right)$ is the entropy of the bipartite subsystem formed by the two modes j' and j'' . On the other hand, $f\left(\sqrt{\epsilon^{j'j''}}\right)$ represents the entropy of the j' -mode after performing a Gaussian measurement on the j'' -mode, where the measurement is chosen to minimize this quantity. In what follows, we shall denote by D^{mo_1} (respectively. D^{mo_2}) the Gaussian quantum discord between the mechanical mode m and the optical mode o_1 (respectively. o_2). Similarly, $D^{o_1o_2}$ stands for the Gaussian quantum discord between the two optical modes o_1 and o_2 .

4.2 Non-classical correlations far beyond entanglement

4.2.1 Gaussian quantum discord versus the thermal effect

The robustness of the different pairwise Gaussian quantum discord on the mechanical thermal bath temperature T and for various values of the squeezing parameters r is illustrated in Fig. 5. In order to compare the behavior of the entanglement (Fig. 2) and the Gaussian quantum discord (Fig. 5) under the thermal effects, we have fixed the parameters as the same as in (Fig. 2). The panels (a), (b) and (c) show that the three Gaussian quantum discords D^{mo_1} , D^{mo_2} and $D^{o_1o_2}$ remain non zero whatever the value of r as well as for high values of the temperature T . Next, comparing the results which illustrated in Figs. 2 and 5, it is clear that unlike the three bipartite entanglements $m - o_1$, $m - o_2$ and $o_1 - o_2$, the three Gaussian quantum discords D^{mo_1} , D^{mo_2} and $D^{o_1o_2}$ do not undergo the sudden

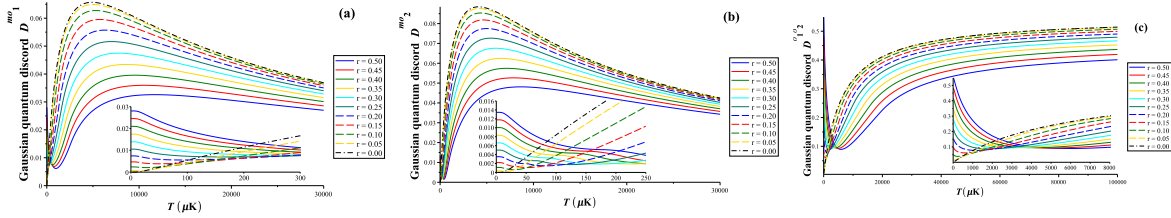


Figure 5: Plots of the three Gaussian quantum discords D^{mo_1} (panel (a)), D^{mo_2} (panel (b)) and $D^{o_1o_2}$ (panel (c)) versus the thermal bath temperature T of the movable mirror and for various values of the squeezing parameter r . The parameters are the same as in Fig. 2. The nonzero asymptotic values of D^{mo_1} , D^{mo_2} and $D^{o_1o_2}$ which corresponding to the case where the whole system is fully separable (see Fig. 2 where $\eta_{mo_1}^- > 1/2$, $\eta_{mo_2}^- > 1/2$ and $\eta_{o_1o_2}^- > 1/2$ for a given squeezing r), confirm the existence of the simultaneous quantumness of correlations in the three subsystems. Non-classicality of the two hybrid subsystems (respectively. the purely optical subsystem) can be observed for temperatures more than $T = 0.03K$ (respectively. $T = 0.1K$). Interestingly enough, the simultaneous reduction of D^{mo_1} and D^{mo_2} from $T \approx 5mK$ is clearly accompanied by the enhancement of $D^{o_1o_2}$. These opposites behaviors can be explained by the purely quantum correlations transfer from the two hybrid subsystems to the homogeneous optical subsystem by means of the movable mirror.

death and remain non zero even for large values of the temperatures T as expected. This reflects the robust character of the Gaussian quantum discord against strong thermal noise. More important, non-classicality of the two hybrid subsystems is significantly nonzero and persists for temperatures up to $0.03K$. Whereas, the quantumness of correlations can be detected more than $T = 0.1K$ in the purely optical subsystem, which is almost of the same order of magnitude that has been observed in Ref [13] for a purely mechanical system. Interestingly enough, Fig. 5 shows that, the Gaussian quantum discords D^{mo_1} and D^{mo_2} start to decay asymptotically with T from $T \approx 5mK$ (see panels (a) and (b) in Fig. 5). On the other hand, the amount of the Gaussian quantum discord $D^{o_1o_2}$ monotonically increases with T also from $T \approx 5mK$ (see panel (c) in Fig. 5), which is a surprising quantum correlations behavior against thermal effects. This result can be explained quantitatively by the purely quantum correlations transfer from the two hybrid subsystems to the homogeneous optical by mediation of the movable mirror shared between the two cavities.

4.2.2 Gaussian quantum discord versus the squeezing effect

The influence of the squeezing on the three Gaussian quantum discords D^{mo_1} , D^{mo_2} and $D^{o_1o_2}$ and for different amounts of the dimensionless optomechanical cooperativity \mathcal{C}_1 is illustrated in Fig. 6. The plots are done by fixing the parameters similarly to ones used to obtain the results reported in Fig. 3. As seen in Fig. 6, the three Gaussian quantum discords D^{mo_1} , D^{mo_2} and $D^{o_1o_2}$ exhibit a resonance like behavior with respect to the squeezing parameter r for a given value of \mathcal{C}_1 . This interesting result means that by controlling the level of the squeezing, one can reach the situation where the two considered modes are maximally discordant. Furthermore, we remark also that when

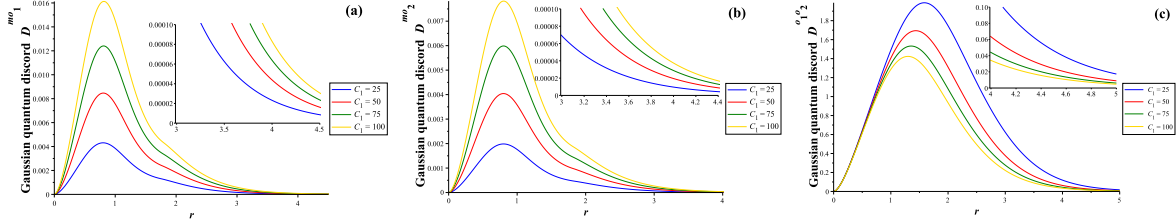


Figure 6: The three Gaussian quantum discords $D^{m o_1}$ (panel (a)), $D^{m o_2}$ (panel (b)) and $D^{o_1 o_2}$ (panel (c)) against the squeezing parameter r and for different values of the optomechanical cooperativity \mathcal{C}_1 ($\mathcal{C}_2 = 2\mathcal{C}_1$). The parameters are the same as in Fig. 3. The three functions $D^{m o_1}$, $D^{m o_2}$ and $D^{o_1 o_2}$ exhibit a resonance like behavior with respect to the squeezing r . Comparing the panels (a), (b) and (c) in this figure with their corresponding in Fig. 3, we can see clearly that when the three subsystems are completely separable ($\eta_{m o_1}^- > 1/2$, $\eta_{m o_2}^- > 1/2$ and $\eta_{o_1 o_2}^- > 1/2$ for a given value of \mathcal{C}_1), non-classical correlations can be observed simultaneously in the three subsystems ($D^{m o_1} > 0$, $D^{m o_2} > 0$ and $D^{o_1 o_2} > 0$) even for squeezing values more than $r = 4.5$ (see the insets in Fig. 6).

the whole system is straightforwardly separable (see for example the case in Fig. 3 which corresponds to $\mathcal{C}_1 = 25$ and $r > 3.5$), the three Gaussian quantum discords $D^{m o_1}$, $D^{m o_2}$ and $D^{o_1 o_2}$ are asymptotically non-zero. This reflects the simultaneous existence of the quantumness of correlations in the three optomechanical subsystems even for squeezing values upper to $r = 4.5$ (see the three insets in Fig. 6).

4.2.3 Gaussian quantum discord versus the optomechanical coupling

Finally, we study the dependence of the three Gaussian quantum discords $D^{m o_1}$, $D^{m o_2}$ and $D^{o_1 o_2}$ with the dimensionless optomechanical cooperativity \mathcal{C}_1 . The resulting behavior is presented in the panels (a), (b) and (c) of Fig. 7 for various amounts of the squeezing parameters r . As illustrated

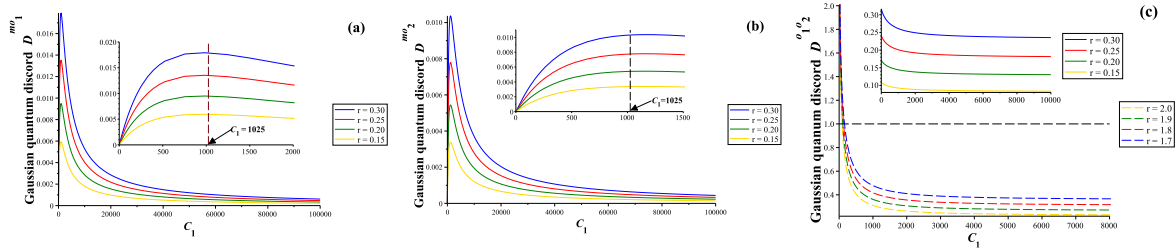


Figure 7: The three Gaussian quantum discords $D^{m o_1}$ (panel (a)), $D^{m o_2}$ (panel (b)) and $D^{o_1 o_2}$ (panel (c)) against the dimensionless optomechanical cooperativity \mathcal{C}_1 ($\mathcal{C}_2 = 2\mathcal{C}_1$). Different values of the squeezing parameter r have been used. The parameters are the same as in Fig. 4. For a given squeeze parameter r , the situation where $\eta_{j' j''}^- > 1/2$ (see Fig. 4) and $D^{j' j''} > 0$ (with $j' \neq j'' = o_1, o_2, m$), witnesses the existence of the quantumness of correlations in the state of the two considered modes j' and j'' .

in Fig. 7, for a given squeeze parameter r , the three bipartite Gaussian quantum discords $D^{m o_1}$,

D^{mo_2} and $D^{o_1o_2}$ are always non-zero (except $\mathcal{C}_1 = 0$ in panels (a) and (b)) regardless the coupling regime. It is also remarkable that in the two hybrid subsystems, the corresponding Gaussian quantum discord D^{mo_1} and D^{mo_2} are always maximal around $\mathcal{C}_1 \approx 1025$ whatever the squeezing parameter r (see the insets of panels (a) and (b) in Fig. 7). It follows that one can reach the maximum amount of the Gaussian quantum discord in the two hybrid subsystems by a judicious tuning of the physical parameters determining the optomechanical cooperativity (see Eq. (31)). Finally, comparing the behavior of the $j' - j''$ entanglement quantified by $\eta_{j',j''}^-$ and the corresponding Gaussian quantum discord $D^{j'j''}$ (with $j' \neq j'' = o_1, o_2, m$) under the effect of either T , r or \mathcal{C}_1 , we remark that: (i) for regions where the Gaussian quantum discord $D^{j'j''}$ is greater than 1, the two modes j' and j'' are entangled ($\eta_{j',j''}^- < 1/2$) and (ii) the Gaussian quantum discord can be less than 1 for both entangled and separable states of the two considered modes j' and j'' , which is in agreement with the proprieties of the Gaussian quantum discord [10, 11].

5 Concluding Remarks

To summarize, both entanglement and Gaussian quantum discord have been studied in a tripartite optomechanical setup (fed by squeezed light) comprising two optical cavities modes and a single mechanical mode. Using a linearized fluctuations analysis under the Markovian process, the 6×6 covariance matrix encoding the essential of the correlations between the different modes, is derived in the resolved-sideband regime. For entanglement characterization, we used the Simon criterion. In order to capture the quantumness of correlations, the Gaussian quantum discord is evaluated employing the method reported in [10, 11, 49]. The entanglement and the Gaussian quantum discord of three different bipartite subsystems have been evaluated as functions of the thermal bath temperature T , the squeezing parameter r and also the optomechanical coupling \mathcal{C}_1 . For an experimentally accessible parameter regime, we showed that it is possible to transfer the quantum correlations from the two-mode squeezed light to the system, creating simultaneous three bipartite optomechanical entanglements. It was further seen that under different circumstance, the purely optical subsystem exhibits more intricacy in comparison with the two hybrid subsystems. As expected, the three bipartite Gaussian quantum discords are shown more resilient against the destructive effects. More important, they are always nonzero even for extremal limiting situations as higher temperature T , large value of the squeezing r and also for both strong coupling ($\mathcal{C}_1 \gg 1$) and weak coupling ($\mathcal{C}_1 \ll 1$). In general, under various conditions, the quantumness of correlations has been detected simultaneously in the three bipartite subsystems over a very wide range of the parameters characterizing the environment and the system. Finally, one should recognize that our study in this two-mode optomechanical system is limited to pairwise quantum correlations. This is essentially due to the fact the characterization of entanglement in multipartite quantum systems remains a complex and open issue. However, we think that the tripartite entanglement classification given in Ref [64], which provides a necessary and sufficient criterion based on the nonpositive partial transposition [65], can be used as an alternative

way to deal with entanglement in the case of tripartite continuous variables Gaussian states. Also, it will be important to consider the balance of pairwise quantum correlations in the tripartite optomechanical system considered here in the spirit of the ideas developed recently in [8]. We hope to report on these issues in a forthcoming works.

References

- [1] M. A. Nielsen and I. L. Chuang, *Quantum Computation and Quantum Information* (Cambridge: Cambridge University Press).
- [2] R. Simon, *Phys. Rev. Lett.* **84** (2000) 2726.
- [3] L. M. Duan, G. Giedke, J. I. Cirac and P. Zoller, *Phys. Rev. Lett.* **84** (2000) 2722.
- [4] G. Vidal and R. F. Werner, *Phys. Rev. A* **65** (2002) 032314.
- [5] S. Mancini, V. Giovannetti, D. Vitali and P. Tombesi, *Phys. Rev. Lett.* **88** (2002) 120401.
- [6] G. Giedke, M. M. Wolf, O. Kruger, R. F. Werner and J. I. Cirac, *Phys. Rev. Lett.* **91** (2003) 107901.
- [7] G. Adesso, A. Serafini and F. Illuminati, *Phys. Rev. A* **70** (2004) 022318.
- [8] S. Olivares and M. G. A. Paris, *Int. J. Mod. Phys. B* **27** (2013) 1345024.
- [9] H. Ollivier and W. H. Zurek, *Phys. Rev. Lett.* **88** (2001) 017901; L. Henderson and V. Vedral, *J. Phys. A* **34** (2001) 6899.
- [10] G. Adesso and A. Datta, *Phys. Rev. Lett.* **105** (2010) 030501.
- [11] P. Giorda and M. G. A. Paris, *Phys. Rev. Lett.* **105** (2010) 020503.
- [12] S. Tesfa, *Optics Communications* **285** (2012) 830; J. Doukas, E. G. Brown, A. Dragan and R. B. Mann, *Phys. Rev. A* **87** (2013) 012306; A. Isar, *Open Sys. Inf. Dynamics*, **18** (2011) 175; L. Mazzola and M. Paternostro, *Nature Scientific Reports* **1** (2011) 199.
- [13] L. Mazzola and M. Paternostro, *Phys. Rev. A* **83** (2011) 062335.
- [14] A. Isar, *Physica Scripta, T* **147** (2012) 014015; J. N. Freitas and J. P. Paz, *Phys. Rev. A* **85** (2012) 032118.
- [15] A. Farace, F. Ciccarello, R. Fazio and V. Giovannetti, *Phys. Rev. A* **89** (2014) 022335.

- [16] S. Campbell, T. J. G. Apollaro, C. D. Franco, L. Banchi, A. Cuccoli, R. Vaia, F. Plastina and M. Paternostro, *Phys. Rev. A* **84** (2011) 052316; C. Benedetti, F. Buscemi, P. Bordone and M. G. A. Paris, *Int. J. Quant. Inf.* **10** (2012) 1241005; A. Auyuanet and L. Davidovich, *Phys. Rev. A* **82** (2010) 032112.
- [17] R. Vasile, P. Giorda, S. Olivares, M. G. A. Paris and S. Maniscalco, *Phys. Rev. A* **82** (2010) 012313.
- [18] E. Verhagen, S. Deléglise, S. Weis, A. Schliesser and T. J. Kippenberg, *Nature* **482** (2012) 63; A. Mari and J. Eisert, *Phys. Rev. Lett.* **108** (2012) 120602.
- [19] O. Romero-Isart, A. C. Pflanzer, F. Blaser, R. Kaltenbaeck, N. Kiesel, M. Aspelmeyer and J. I. Cirac, *Phys. Rev. Lett.* **107** (2011) 020405; K. Stannigel, P. Komar, S. J. M. Habraken, S. D. Bennett, M. D. Lukin, P. Zoller and P. Rabl, *Phys. Rev. Lett.* **109** (2012) 013603.
- [20] M. Aspelmeyer, T. J. Kippenberg and F. Marquardt, *Rev. Mod. Phys.* **86** (2014) 1391.
- [21] C. Genes, A. Mari, D. Vitali and P. Tombesi, *Adv. At. Mol. Opt. Phys.* **57** (2009) 33.
- [22] F. Marquardt, J. P. Chen, A. A. Clerk and S. M. Girvin, *Phys. Rev. Lett.* **99** (2007) 093902.
- [23] M. Bhattacharya and P. Meystre, *Phys. Rev. Lett.* **99** (2007) 073601.
- [24] S. Bose, K. Jacobs and P. L. Knight, *Phys. Rev. A* **56** (1997) 4175; W. Marshall, C. Simon, R. Penrose and D. Bouwmeester, *Phys. Rev. Lett.* **91** (2003) 130401.
- [25] J. Zhang, K. Peng and S. L. Braunstein, *Phys. Rev. A* **68** (2003) 013808.
- [26] V. B. Braginsky and F. Ya Khalili, *Quantum Measurements*, Cambridge University Press, Cambridge, (1992); J. Mertz, O. Marti and J. Mlynek, *Appl. Phys. Lett.* **62** (1993) 2344.
- [27] J. Eisert, M. B. Plenio, S. Bose and J. Hartley, *Phys. Rev. Lett.* **93** (2004) 190402; S. Mancini, D. Vitali, V. Giovannetti and P. Tombesi, *Eur. Phys. J. D* **22** (2003) 417.
- [28] M. Pinard, A. Dantan, D. Vitali, O. Arcizet, T. Briant and A. Heidmann, *Europhys. Lett.* **72** (2005) 747.
- [29] S. Huang and G. S. Agarwal, *New Journal of Physics* **11** (2009) 103044.
- [30] D. Vitali, S. Gigan, A. Ferreira, H. R. Bohm, P. Tombesi, A. Guerreiro, V. Vedral, A. Zeilinger and M. Aspelmeyer, *Phys. Rev. Lett.* **98** (2007) 030405.
- [31] G. Wang, L. Huang, Y. C. Lai and C. Grebogi, *Phys. Rev. Lett.* **112** (2014) 110406; A. Mari and J. Eisert, *New Journal of Physics* **14** (2012) 075014.
- [32] J. El Qars, M. Daoud and Ahl Laamara, *Int. J. Quant. Inform.* **13** (2015) 1550041.

- [33] V. Giovannetti, S. Mancini and P. Tombesi, *Europhys. Lett.* **54** (2001) 559.
- [34] M. Paternostro, D. Vitali, S. Gigan, M. S. Kim, C. Brukner, J. Eisert and M. Aspelmeyer, *Phys. Rev. Lett.* **99** (2007) 250401.
- [35] D. C. Burnham and D. L. Weinberg, *Phys. Rev. Lett.* **25** (1970) 84; Y. H. Shih and C. O. Alley, *Phys. Rev. Lett.* **61** (1988) 2921.
- [36] C. K. Law, *Phys. Rev. A* **51** (1995) 2537.
- [37] V. Giovannetti and D. Vitali, *Phys. Rev. A* **63** (2001) 023812.
- [38] C. W. Gardiner and P. Zoller, *Quantum Noise*, (Springer, Berlin, 2000), p. 71.
- [39] C. W. Gardiner, *Phys. Rev. Lett.* **56** (1986) 1917.
- [40] D. F. Walls and G. J. Milburn, 1998 *Quantum Optics* (Berlin: Springer); C. Fabre, M. Pinard, S. Bourzeix, A. Heidmann, E. Giacobino and S. Reynaud, *Phys. Rev. A* **49** (1994) 1337.
- [41] S. Mancini and P. Tombesi, *Phys. Rev. A* **49** (1994) 4055.
- [42] M. Paternostro, S. Gigan, M. S. Kim, F. Blaser, H. R. Bohm and M. Aspelmeyer, *New Journal of Physics* **8** (2006) 107.
- [43] L. Tian and H. Wang, *Phys. Rev. A* **82** (2010) 053806; Y. -D. Wang and A. A. Clerk, *Phys. Rev. Lett.* **108** (2012) 153603; E. A. Sete, H. Eleuch and C. H. R. Ooi, *J. Opt. Soc. Am. B* **31** (2014) 2821.
- [44] Y. D. Wang, S. Chesi and A. A. Clerk, *Phys. Rev. A* **91** (2015) 013807.
- [45] T. P. Purdy, P. -L. Yu, R. W. Peterson, N. S. Kampel and C. A. Regal, *Phys. Rev. X* **3** (2013) 031012.
- [46] S. Gröblacher, K. Hammerer, M. R. Vanner and M. Aspelmeyer, *Nature* **460** (2009) 724.
- [47] E. X. DeJesus and C. Kaufman, *Phys. Rev. A* **35** (1987) 5288.
- [48] Sh. Barzanjeh, D. Vitali, P. Tombesi and G. J. Milburn, *Phys. Rev. A* **84** (2011) 042342.
- [49] S. Olivares, *Eur. Phys. J. Special Topics* **203** (2012) 3.
- [50] G. Adesso, S. Ragy and A. R. Lee, *Open Systems & Information Dynamics* **21** (2014) 1440001.
- [51] C. Genes, A. Mari, P. Tombesi and D. Vitali, *Phys. Rev. A* **78** (2008) 032316.
- [52] A. Ferraro, M. G. A. Paris, A. Allevi, A. Andreoni, M. Bondani and E. Puddu, *J. Opt. Soc. Am. B* **21** (2004) 1241.

- [53] B. Rogers, M. Paternostro, G. M. Palma and G. D. Chiara, *Phys. Rev. A* **86** (2012) 042323; G. De Chiara, M. Paternostro and G. M. Palma, *Phys. Rev. A* **83** (2011) 052324.
- [54] C. Genes, D. Vitali and P. Tombesi, *New Journal of Physics* **10** (2008) 095009; C. Genes, D. Vitali and P. Tombesi, *Phys. Rev. A* **77** (2008) 050307(R).
- [55] N. Aggarwal, K. Debnath, S. Mahajan, A. B. Bhattacharjee and M. Mohan, *Int. J. Quant. Inf.* **12** (2014) 1450024; M. Abdi and A. R. Bahrampour, *Phys. Lett. A* **376** (2012) 2955; Sh. Barzanjeh, M. H. Naderi and M. Soltanolkotabi, *Phys. Rev. A* **84** (2011) 063850; Z. C. Shi, Y. Xia and J. Song, *Quantum Inf Process*, **12** (2013) 3179; E. Wu, X. G. Han, *Int. J. Theor. Phys* **52** (2013) 2607.
- [56] M. Paternostro, L. Mazzola and J. Li, *J. Phys. B: At. Mol. Opt. Phys.* **45** (2012) 154010.
- [57] J. Eisert and M. B. Plenio, *Int. J. Quant. Inf.* **1** (2003) 479.
- [58] J. Eisert, Ph.D. thesis, University of Potsdam, 2001.
- [59] K. W. Murch, K. L. Moore, S. Gupta and D. M. Stamper-Kurn, *Nat. Phys.* **4** (2008) 561.
- [60] M. Daoud and R. A. Laamara, *Phys. Lett. A* **376** (2012) 2361; A. AlQasimi and D. F. V. James, *Phys. Rev. A* **77** (2008) 012117.
- [61] Y. -D. Wang and A. A. Clerk, *Phys. Rev. Lett.* **110** (2013) 253601.
- [62] L. A. Correa, A. A. Valido and D. Alonso, *Phys. Rev. A* **86** (2012) 012110.
- [63] A. Serafini, F. Illuminati and S. D. Siena, *J. Phys. B: At. Mol. Opt. Phys.* **37** (2004) L21.
- [64] G. Giedke, B. Kraus, M. Lewenstein and J. I. Cirac, *Phys. Rev. A* **64** (2001) 052303.
- [65] R. F. Werner and M. M. Wolf, *Phys. Rev. Lett.* **86** (2001) 3658.